Geological Lineament Pattern and Geomorphic Indices Characteristic Related to Geothermal Manifestation Appearance: A Case Study from Gunung Talang District and Its Surroundings, Solok Regency, West Sumatra Province, Indonesia

Jordi Andrifa, Nana Sulaksana, Dewi Gentana, Murni Sulastri

Faculty of Geological Engineering, Universitas Padjadjaran, Sumedang, Indonesia

ABSTRACT

The study area is located in Gunung Talang District and its surroundings, Solok Regency, West Sumatra Province, Indonesia. This area has a potential volcanic geothermal system and is generally covered by the Quarternary rocks which are deformed due to the tectonic activity of the Sumatran Fault System. Geological structure traces are not well preserved in such an area. This study aims to determine the geological lineament pattern associated with geological structure, the geomorphic indices characteristic related to the tectonic activity and rock permeability, and the geothermal manifestation appearance based on these two factors. Geological lineament pattern is identified using the remote sensing method. Geomorphic indices characteristic is calculated through the quantitative analysis of bifurcation ratio (R_b), drainage density (D_d), mountain front sinuosity (S_{mf}), and lineament density (L_d). Geothermal manifestation appearance is evaluated through geospatial analysis using the overlay method on the geological lineament pattern and the geomorphic indices characteristic, which are then correlated with the distribution of geothermal manifestations. The main geological lineament patterns associated with the geological structures in the study area are north-northwest–south-southeast (NNW-SSE) and northeast-southwest (NE-SW). These lineament patterns indicate synthetic and antithetic strike-slip faults around the Sumani Segment of Sumatran Fault System successively. The geomorphic indices characteristics imply deformed areas (R_b values: 1.14-5.45), rough (D_d values: 2.00-2.66 km/km²), moderate (D_d values: 3.14-4.00 km/km²), and slightly fine landform textures (D_d values: 4.32-5.51 km/km²), active (S_{mf} values: 1.05-1.64) and moderate to slightly active tectonisms (S_{mf} values: 1.74-2.52), low (L_d values: 0.00-0.84 km^{-1}), moderate (L_d values: 0.84-1.68 km^{-1}), and high lineament densities (L_d values: 1.68-2.52 km^{-1}) over the study area. The geothermal manifestations in the study area are

divided into four groups based on their appearance characteristics, namely group I (Songsang and Garara hot springs), group II (Padang Damar, Bukit Gadang, and Batu Bajanjang hot springs), group III (Bukit Kili and Bawah Gunuang hot springs), and group IV (Gabuo Atas and Bawah Betung hot springs).

Keywords: Geological Lineament, Geomorphic Indices, Geothermal Manifestation, Gunung Talang

I. INTRODUCTION

Geothermal energy is the energy derived from heat sources beneath the earth's surface. This energy can be used as a renewable and eco-friendly source for producing electricity [1]. As a country with the largest geothermal energy resource potential, Indonesia has more than 29,000 MW or approximately 40% of the world geothermal resources potential [2]. This potential is an implication of the complex interactions between the Indo-Australian, Eurasian, and Pacific Plates that have resulted in volcanic activity and major faults in Indonesia [3]. By the 13,470 MW geothermal potential for electricity generation, Sumatra Island has the largest accumulative geothermal potential over the other islands in Indonesia [4]. Gunung Talang - Bukit Kili is an area that has geothermal resource potential on this island, which is estimated to have the potential for electricity generation of 65 MW [5]. The study area is administratively located in Gunung Talang and its surroundings, Solok Regency, West Sumatra Province, Indonesia (Figure. 1).

According to [6], the study area is relatively covered by the Quaternary volcanic rocks such as the Undifferentiated Volcanic Products (QTau), Welded Tuff (QTwt), Andesite of Gunung Talang (Qatg), and Alluvial Fans (Qf) (Figure 2). In addition, there are a few pre-Tertiary to Tertiary age rocks such as the Slate and Shale Member of Tuhur Formation (Trts) and Andesite to Basalt (Ta) in the northwestern part of the study area. The study area is regionally influenced by tectonic activities such as magmatic arc and the active Sumatran Fault System [7]. Based on its geomorphic characteristic, this area is deformed by the Sumani Segment of the Sumatran Fault [8]. Based on the structural geology aspect, graben structures are common in the study area. Therefore, the geothermal system in the study area can be classified as a graben-type geothermal system [9].
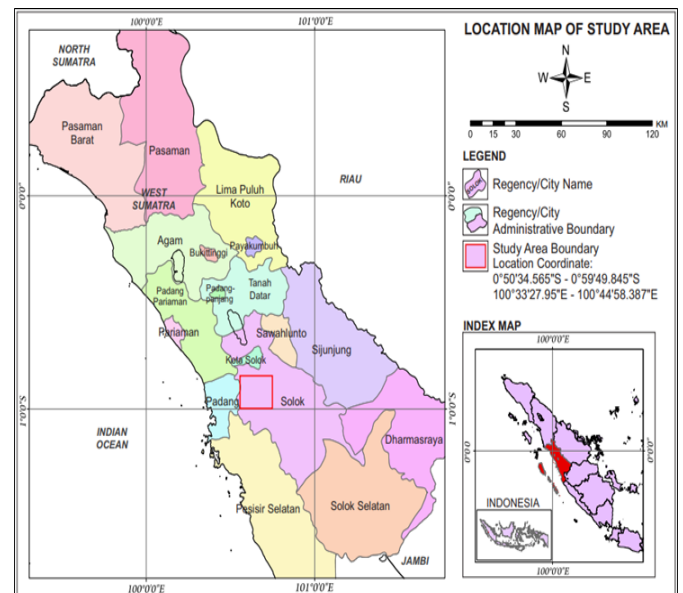

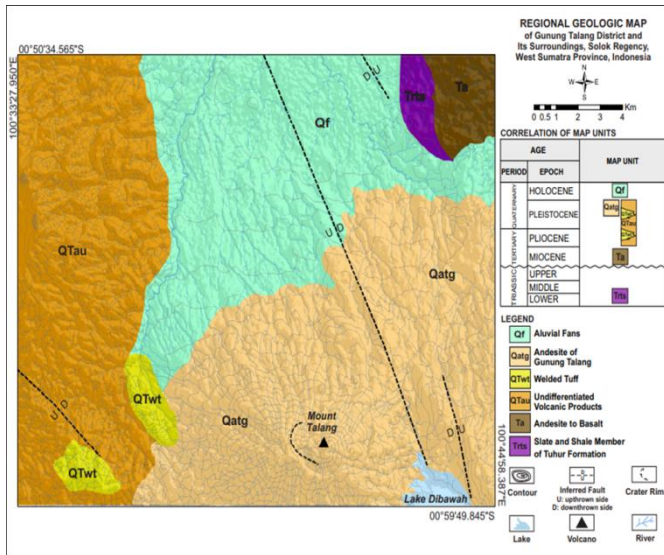
Figure 1: Location map of study area

Figure 2: Regional geologic map of study area (modified from [6])

The existence of geothermal resources is usually indicated by the appearance of geothermal surface manifestations as a result of the heat propagation from the subsurface and the flow of geothermal fluid to the surface through the rock fractures [10]. The data gathered in [11] and [12] suggest that thirteen geothermal manifestation points in the study area are included as a hot spring type. Fracture is a geological structure that can be caused by rock deformation due to tectonic activity and igneous intrusion. It creates a permeable zone that can be a pathway for the flow of geothermal fluid from the reservoir to the surface. This permeable zone has proven to be a productive well drilling target in geothermal exploration and exploitation activities [13], [14] in [15].

Structural lineament analysis can provide an overview of local tectonic features and information about possible regional tectonic evolution [16]. The lineament pattern is useful for identifying the pattern of main geological structure which affects the distribution of geothermal manifestations [17]. A quantitative approach based on the geomorphic indices is used to increase the accuracy of geomorphological analysis, specifically in identifying tectonic activity and rock permeability in areas with Quaternary volcanic landforms. This approach is used because the traces of geological structures are not well

preserved in Quaternary volcanic rocks, which are not yet fully compacted [18]. This study aims to evaluate geological lineament patterns associated with geological structures, tectonic activity, and rock permeability, especially around the appearance of geothermal manifestations, which indicate the geothermal potential in the study area.

II. METHODS AND MATERIAL

This study is conducted using data obtained from the Indonesian Terrain Map [19], Advanced Spaceborne Thermal Emission and Reflection Radiometer Global Digital Elevation Model (ASTER GDEM) [20], and previous researches. Geological lineament pattern is identified using remote sensing methods. Identification of geomorphic indices characteristic is carried out through quantitative analysis based on four parameters, namely bifurcation ratio (R_b), drainage density (D_d), mountain front sinuosity (S_{mf}), and lineament density (L_d). The appearance of geothermal manifestation is evaluated through geospatial analysis using the overlay method on the geological lineament pattern and the geomorphic indices characteristic which are then correlated with geothermal manifestation distribution.

A. Geological Lineament Pattern

The expression of geological lineament on the surface due to the reactivation of subsurface geological structures can reflect the lineament zones associated with broad geological structures. This feature can be identified at a certain edge that has a subtle brightness difference in the image. It can reflect the straight stream and valley, alignment in depressions, abrupt topographic changes, soil tonal changes, and alignment in vegetations [21] in [22]. Identification of this feature is carried out through shaded topographic relief created using certain apparent sun positions with a 45° azimuth increment starting from the north. It aims to identify the lineament in all directions. Lowering vertical sun angle and superimposing

detailed topographic contours can help to identify vague lineament [14]. Identified lineaments are depicted on a rose diagram to illustrate the main geological lineament patterns in the study area [17]. Structural patterns analysis in satellite imagery shows that lineament pattern can be classified into different groups based on their orientation [23]. The orientation and sense of strain of geological structures in the strike-slip fault zone associated with the *en echelon* arrangement are consistently arranged with respect to the principle displacement zone (PDZ) [24]. Hence, the structural pattern can be used for further interpretation of the geological structure by recognizing the PDZ in the study area.

B. Geomorphic Indices

1) Bifurcation Ratio (R_b): Bifurcation ratio (R_b) is the ratio between the number of a certain order stream segment ($\sum N_u$) and a higher-order stream segment ($\sum N_{u+1}$). The Rb value is obtained using the following equation:

$$R_b = \sum N_u / \sum N_{u+1} \text{....................} (1)$$

The watershed with a value of $R_b < 3.0$ or $R_b > 5.0$ is indicated to have undergone deformation which is controlled by the tectonic activity, whereas the watershed with an R_b value of 3.0–5.0 indicates that the area is not deformed by the tectonic activity [25] in [18].

2) Drainage Density (D_d): Drainage density (D_d) is the ratio between the total length of streams ($\sum L$) and the watershed or sub-watershed area (A). The D_d value is calculated using the following equation [26]:

$$D_d = \sum L / A \text{....................} (2)$$

The D_d value is useful for identifying the texture of Quarternary volcanic landform, namely very coarse (D_d values: 0.00-1.37 km/km²), coarse (D_d values: 1.38-2.75 km/km²), moderate (D_d values: 2.76-4.13 km/km²), slightly fine (D_d values: 4.14-5.51 km/km²), fine (D_d values: 5.52-6.89 km/km²), and very fine textures (D_d values: 6.90-8.27 km/km²) [27] in [18]. The low D_d values

associated with coarse to medium landform textures indicate the presence of permeable rock under a watershed [28]. Meanwhile, the high D_d value indicates impermeable rock beneath a watershed with a large number of streamflows on the surface [18].

3) Mountain Front Sinuosity (S_{mf}): Mountain front sinuosity (S_{mf}) is a geomorphic index that explains the relationship between tectonic activity that forms a straight mountain front and the erosion process of a river that intersects mountain front [29] in [30]. The value of the mountain front sinuosity (S_{mf}) can be obtained from the comparison between the length of the mountain front segment (L_{mf}) and the length of the projected mountain front segment (L_s), as expressed on the following equation:

$$S_{mf} = L_{mf} / L_s \text{....................} (3)$$

The value of S_{mf} is useful to identify the tectonic activity such as active tectonism (S_{mf} values: 1.2-1.6), moderate to slightly active tectonism (S_{mf} values: 1.8-3.4), and tectonically inactive (S_{mf} values: 2.0-7.0) [29] in [31].

4) Lineament Density (L_d): Lineament density (L_d) is the ratio between the total length of lineament (F) and the area of a calculation grid (A). Faults and fractures as products of tectonic activity can be used to identify geothermal fields using this parameter. A high lineament density indicates the presence of a permeable zone associated with geothermal reservoirs. The L_d value is calculated using the following equation:

$$L_d = F / A \text{....................} (4)$$

The calculation of lineament density uses a gridding system with a grid size of 1x1 km² as the area of calculation to obtain the lineament length per unit area (km⁻¹) at the centre point of each grid. The L_d value of each grid is useful to construct the contours illustrating the lineament density of an area [13]. Previous research around Mount Rendingan in Lampung Province, Indonesia showed areas with low lineament

density (L_d values < 1.00 km^{-1}), moderate lineament density (L_d values: 1.00-2.00 km^{-1}), and high lineament density (L_d values: 2.00-3.00 km^{-1}) [32].

III. RESULTS AND DISCUSSION

A. Geological Lineament Pattern

Lineament pattern depiction on the rose diagram in the map of geological lineament pattern shows that relatively there are two main patterns in the study area, namely the northwest-southeast (NW-SE) and northeast-southwest (NE-SW) patterns (Figure 3). The northwest-southeast (NW-SE) lineament pattern indicates a strike-slip fault in the principle displacement zone (PDZ) and synthetic strike-slip faults with north-northwest–south-southeast (NNW-SSE) and northwest-southeast (NW-SE) patterns. The northeast-southwest (NE-SW) lineament pattern indicates antithetic strike-slip faults with a northeast-southwest (NE-SW) and north-northeast–south-southwest (NNE-SSW) patterns. Moreover, there are circular patterns associated with crater or caldera remnants that indicate past volcanic activity.
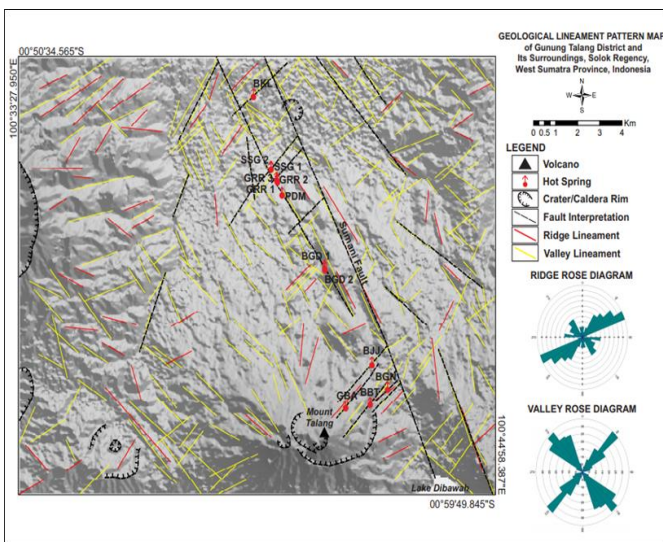

Figure 3: Geological lineament pattern map and rose diagram of study area show the main lineament patterns, namely northwest-southeast (NW-SE) and northeast-southwest (NE-SW), as the indication of

structural patterns associated with the appearance of geothermal manifestations in the study area

B. Geomorphic Indices

1) Bifurcation Ratio (R_b): The bifurcation ratio of seventeen sub-watersheds in the study area has the R_b values range from 1.14 to 5.45 (Table 1). There are seven sub-watersheds in the Batang Sumani watershed with the R_b values range from 1.14 to 2.17. In the Air Bartumbuh watershed, there are five sub-watersheds with the R_b values range from 1.78 to 5.01. In the Batang Lembang watershed, there are five sub-watersheds with the R_b values range from 1.68 to 5.45. Based on the classification of R_b values [25] in [18], all sub-watersheds in the study area are inferred to have undergone deformation controlled by the tectonic activity.

TABLE I
THE RESULT OF BIFURCATION RATIO (R_b)
CALCULATION AND ITS SIGNIFICATION

Watershed	Sub-Water-shed	Segment Number of Stream Order					R_b Value				R_b Mean Value	Signification
		1st	2nd	3rd	4th	5th	1-2	2-3	3-4	4-5		
Batang Sumani	SW 1	402	196	116	50	37	2.05	1.69	2.32	1.35	1.85	Deformed
	SW 2	293	131	97	40	17	2.24	1.35	2.43	2.35	2.09	Deformed
	SW 3	63	42	18			1.50	2.33			1.92	Deformed
	SW 4	22	12	8			1.83	1.50			1.67	Deformed
	SW 5	21	10	8			2.10	1.25			1.68	Deformed
	SW 6	8	7				1.14				1.14	Deformed
	SW 13	29	17	8	3		1.71	2.13	2.67		2.17	Deformed
Air Bartumbuh	SW 7	28	13	9	5		2.15	1.44	1.80		1.80	Deformed
	SW 8	44	19	9	15	1	2.32	2.11	0.60	15.00	5.01	Deformed
	SW 9	21	6	12	4		3.50	0.50	3.00		2.33	Deformed
	SW 14	10	6	3			1.67	2.00			1.83	Deformed
	SW 15	19	11	6			1.73	1.83			1.78	Deformed
Batang Lembang	SW 10	21	8	11			2.63	0.73			1.68	Deformed
	SW 11	23	10		13		2.30				2.30	Deformed
	SW 12	115	60	32	5	18	1.92	1.88	6.40	0.28	2.62	Deformed
	SW 16	24	15	5	4		1.60	3.00	1.25		1.95	Deformed
	SW 17	36	20	13	1		1.80	1.54	13.00		5.45	Deformed

The geothermal manifestations in the study area appear in deformed sub-watersheds with the R_b values ranging from 1.68 to 2.33 and 5.01 (Figure 4). Bukit Kili (BKL) hot spring appears in Sub-Watershed 8 (SW 8) with an R_b value of 5.01. Songsang (SSG), Garara (GRR), and Padang Damar (PDM) hot springs appear in Sub-Watershed 9 (SW 9) with an R_b value of 2.33.

Bukit Gadang (BGD) hot springs appear in Sub-Watershed 14 (SW 14) with an R_b value of 1.83. Batu Bajanjang (BJJ) hot spring appears in Sub-Watershed 10 (SW 10) with an R_b value of 1.68). Bawah Gunuang (BGN), Gabuo Atas (GBA), and Bawah Betung (BBT) hot springs appear in Sub-Watershed 16 (SW 16) with an R_b value of 1.95.
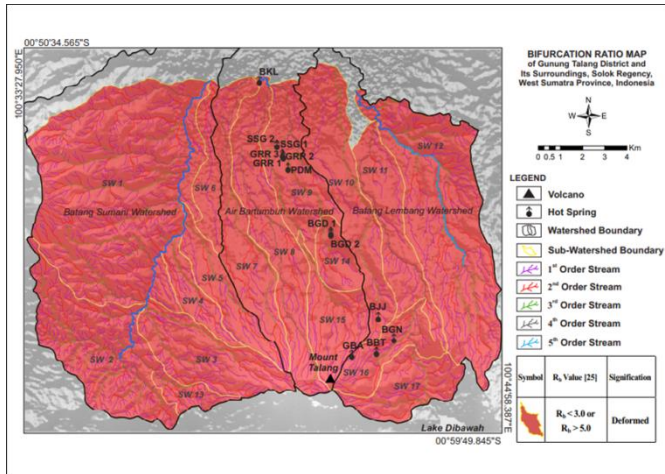

Figure 4: Bifurcation ratio (R_b) map of seventeen sub-watersheds shows the influence of deformation due to the tectonic activity related to the appearance of geothermal manifestation in the study area

2) Drainage Density (D_d): The drainage density of seventeen sub-watersheds in the study area has D_d values range from 2.00 to 5.51 km/km². Based on the textural classification of Quarternary volcanic landform, [27] in [18], a coarse, moderate, and slightly fine landform texture has developed in the study area (Table 2). Batang Sumani watershed with the D_d values ranging from 2.03 to 5.51 km/km² mainly consists of sub-watersheds with a slightly fine landform texture. In comparison, Air Bartumbuh watershed with the D_d values ranging from 2.34 to 3.90 km/km² and Batang Lembang watershed with the D_d values ranging from 2.00 to 4.00 km/km² mainly consist of sub-watersheds with moderate and coarse landform textures. Geothermal manifestations appear in these two watersheds. Based on [18] and [28], a high D_d value indicates low rock

permeability, while a low D_d value indicates high rock permeability. Therefore, it can be seen that the sub-watersheds with a coarse landform texture in the study area (viz., SW 6, SW 9, SW 10, SW 11, and SW 14) are associated with relatively high rock permeability zone, sub-watersheds with a moderate landform texture in the study area (viz., SW 5, SW 7, SW 8, SW 12, SW 15, SW 16, and SW 17) are associated with relatively moderate rock permeability zone, while sub-watersheds with a slightly fine landform texture in the study area (viz., SW 1, SW 2, SW 3, SW 4, and SW 13) are associated with relatively low rock permeability zone.

TABLE II

THE RESULT OF DRAINAGE DENSITY (D_d) CALCULATION AND ITS SIGNIFICATION

Watershed	Sub-Watershed	Total Length of Streams (? L)	Area (A)	Drainage Density (D_d)	Landform Texture
Batang Sumani	SW 1	264.79	61.06	4.34	Slightly Fine
	SW 2	128.44	24.12	5.33	Slightly Fine
	SW 3	67.51	15.05	4.49	Slightly Fine
	SW 4	22.69	5.25	4.32	Slightly Fine
	SW 5	31.44	8.44	3.73	Moderate
	SW 6	11.82	5.82	2.03	Coarse
	SW 13	17.76	3.22	5.51	Slightly Fine
Air Bartumbuh	SW 7	46.36	14.75	3.14	Moderate
	SW 8	66.22	19.36	3.42	Moderate
	SW 9	31.29	13.39	2.34	Coarse
	SW 14	12.87	4.83	2.66	Coarse
	SW 15	38.03	9.74	3.90	Moderate
Batang Lembang	SW 10	38.70	19.37	2.00	Coarse
	SW 11	35.56	13.37	2.66	Coarse
	SW 12	134.35	37.74	3.56	Moderate
	SW 16	33.02	8.25	4.00	Moderate
	SW 17	36.99	9.95	3.72	Moderate

Geothermal manifestations in the study area appear in sub-watersheds with moderate to coarse landform textures (D_d values: 2.00-4.00 km/km² (Figure 5). The geothermal manifestations appeared in the coarse landform texture consist of Songsang (SSG), Garara (GRR), and Padang Damar (PDM) hot springs distributed in Sub-Watershed 9 (SW 9) with a D_d value of 2.34 km/km², Bukit Gadang (BGD) hot springs distributed in Sub-Watershed 14 (SW 14) with a D_d value of 2.66 km/km², and Batu Bajanjang (BJJ)

hot spring located in Sub-Watershed 10 (SW 10) with a D_d value of 2.00 km/km². Meanwhile, the geothermal manifestations appeared in the moderate landform texture consist of Bukit Kili (BKL) hot spring located in Sub-Watershed 8 (SW 8) with a D_d value of 3.42 km/km², Bawah Gunuang (BGN), Gabuo Atas (GBA), and Bawah Betung (BBT) hot springs distributed in Sub-Watershed 16 (SW 16) with a D_d value of 4.00 km/km². Sub-watersheds with a slightly fine landform texture (D_d values: 4.32-5.51 km/km²) are inferred to have a relatively low rock permeability so that it cannot flow the geothermal fluid up to the earth's surface.
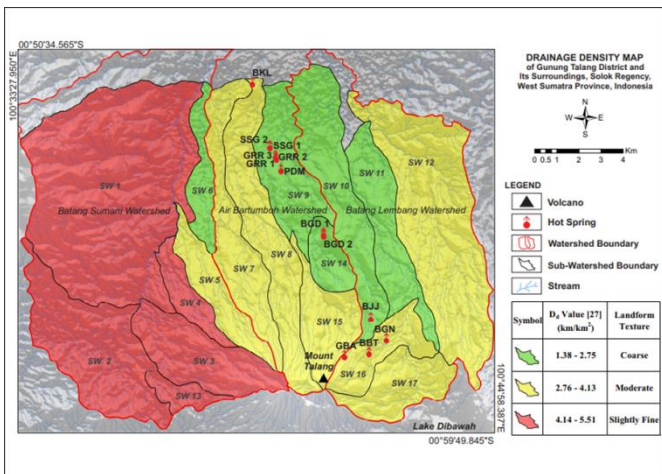
Figure 5: Drainage Density (D_d) map of seventeen sub-watersheds shows that the landform textures associated with the appearance of geothermal manifestation in the study area are the coarse and moderate textures

3) Mountain Front Sinuosity (S_{mf}): The mountain front sinuosity of thirty-eight mountain front segments in the study area has S_{mf} values ranging from 1.05 to 2.52. Based on the classification of S_{mf} value [29] in [31], thirty-three mountain front segments indicate active tectonisms with the S_{mf} values range from 1.05 to 1.64, while five mountain front segments indicate moderate to slightly active tectonisms with the S_{mf} values range from 1.74 to 2.52 (Table 3).

TABLE III
THE RESULT OF MOUNTAIN FRONT SINUOSITY (S_{mf}) CALCULATION AND ITS SIGNIFICATION

No.	L_{mf}	L_s	S_{mf}	Tectonic Activity
1	6.71	2.66	2.52	Moderate to Slightly Active
2	7.34	4.04	1.82	Moderate to Slightly Active
3	3.61	2.35	1.54	Active
4	4.51	2.38	1.90	Moderate to Slightly Active
5	7.43	5.38	1.38	Active
6	3.38	2.40	1.41	Active
7	4.27	2.20	1.94	Moderate to Slightly Active
8	2.93	2.24	1.30	Active
9	5.06	3.10	1.64	Active
10	2.28	1.86	1.23	Active
11	4.03	2.79	1.45	Active
12	3.56	3.12	1.14	Active
13	2.44	1.87	1.30	Active
14	9.37	5.95	1.58	Active
15	2.69	2.17	1.24	Active
16	3.04	2.55	1.19	Active
17	3.73	2.65	1.41	Active
18	8.99	6.83	1.32	Active
19	6.05	4.01	1.51	Active
20	1.53	1.24	1.23	Active
21	2.54	2.20	1.16	Active
22	2.73	2.35	1.16	Active
23	1.73	1.41	1.23	Active
24	2.52	2.04	1.23	Active
25	4.69	2.70	1.74	Moderate to Slightly Active
26	6.51	4.50	1.45	Active
27	4.02	2.62	1.53	Active
28	4.41	3.04	1.45	Active
29	3.96	2.67	1.48	Active
30	7.18	5.14	1.40	Active
31	3.29	2.67	1.23	Active
32	2.31	1.63	1.42	Active
33	1.58	1.21	1.30	Active
34	2.62	2.11	1.24	Active
35	3.63	2.45	1.48	Active
36	3.47	3.01	1.15	Active
37	3.96	3.02	1.31	Active
38	3.24	3.08	1.05	Active

Geothermal manifestations in the study area appear around the mountain front segments,

which indicate active tectonisms with the S_{mf} values ranging from 1.16 to 1.58 (Figure 6). Bukit Kili (BKL) hot spring appears around segment 14 with an S_{mf} value of 1.58. Songsang (SSG) and Garara (GRR) hot springs appear around segment 15 with an S_{mf} value of 1.24. Padang Damar (PDM) hot spring appears in segment 16 with an S_{mf} value of 1.19. Bukit Gadang (BGD) hot 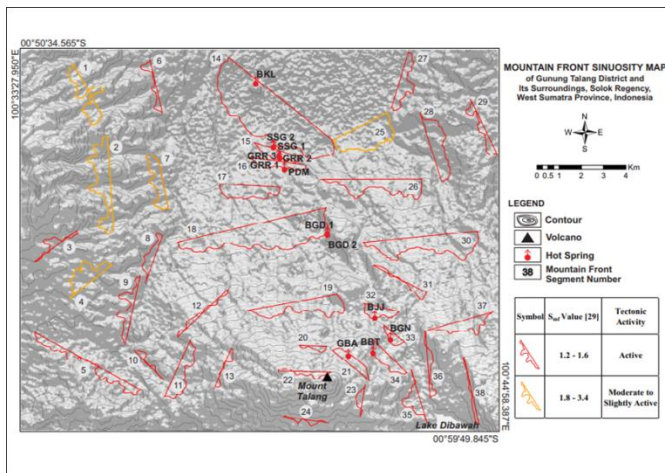springs appear in segment 18 with an S_{mf} value of 1.32. Batu Bajanjang (BJJ) hot spring appears in segment 32 with an S_{mf} value of 1.42. Bawah Gunuang (BGN) hot spring appears in segment 33 with an S_{mf} value of 1.30. Gabuo Atas (GBA) hot spring appears in segment 21 with an S_{mf} value of 1.16. Bawah Betung (BBT) hot spring appears in segment 34 with an S_{mf} value of 1.24.

Figure 6: Mountain front sinuosity (S_{mf}) map of the study area shows the appearance of geothermal manifestations around the mountain front segments indicating active tectonisms

4) Lineament Density (L_d): The lineament density analysis shows the distribution of low to high lineament density zones in the study area with the L_d values ranging from 0.00 to 2.52 km^{-1}. According to [13] and [14], high lineament density indicates the presence of a permeable zone. Therefore it can be seen that the study area consists of: the low lineament density areas associated with relatively low rock permeability zones, which are represented by dark to light green colour (L_d values: 0.00-0.84 km^{-1}); the moderate lineament density areas associated with relatively moderate rock permeability zones, which are represented by light to dark yellow colour (L_d values: 0.84-1.68 km^{-1}); and the high lineament density areas associated with relatively high rock permeability zones, which are represented by light to dark orange colour (L_d values: 1.68-2,52 km^{-1}).

Geothermal manifestations in the study area appear in the moderate to high lineament density areas with the L_d values range between 1.26 and 2.52 km^{-1} (Figure 7). Bukit Kili (BKL), Songsang (SSG), Garara (GRR), and Bawah Gunuang (BGN) hot springs appear in the high lineament density areas with the L_d values range from 1.68 to 2.52 km^{-1}. Meanwhile, Padang Damar (PDM), Bukit Gadang (BGD), Batu Bajanjang (BJJ), Gabuo Atas (GBA), and Bawah Betung (BBT) hot springs appear in the moderate lineament density areas with the L_d values range from 1.26 to 1.68 km^{-1}. The low lineament density areas with the L_d values range between 0.00 and 0.84 km^{-1} is inferred to have a low fault and fracture intensity associated with an impermeable zone that has a low capability to flow the geothermal fluid up to the earth's surface.
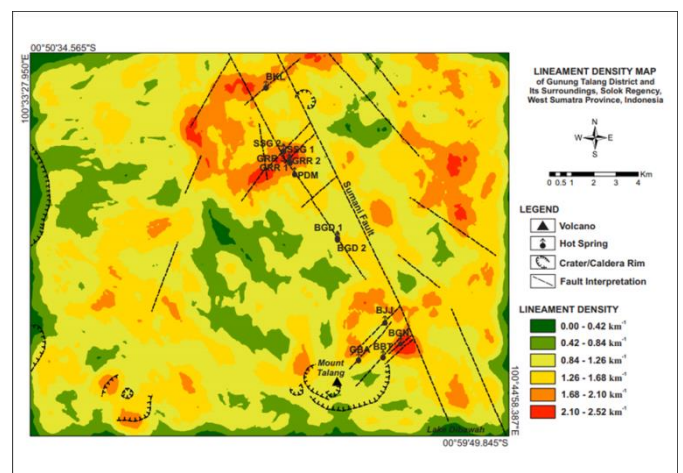

Figure 7: Lineament density (L_d) map of the study area shows the appearance of geothermal manifestations in the moderate to high lineament density areas

C. Geothermal Manifestation Appearance

The analysis of geological lineament pattern shows that the geothermal manifestation appearance in the study area is associated with geological structures that have relatively north-northwest–south-southeast (NNW-SSE) and northeast-southwest (NE-SW) patterns. These structural patterns indicate synthetic and antithetic strike-slip faults developed around the Sumani Segment of Sumatran Fault, which causes rock deformation to form permeable zones that have a high capability to flow the geothermal fluid up to the earth's surface. The calculation of the geomorphic indices using the parameters of the bifurcation ratio (R_b) and the mountain front sinuosity (S_{mf}) shows the similarity on the appearance of geothermal manifestations, which is distributed in the areas that have undergone deformation due to active tectonism. The calculations of drainage density (D_d) and lineament density (L_d) parameters show characteristic variations on the appearance of geothermal manifestations, which are appeared in the areas with moderate to coarse landform textures and medium to high lineament densities, associated with relatively moderate to high rock permeability zones. These findings suggest that the geothermal manifestations in the study area are divided into four groups, namely group I, II, III, and IV (Table 4).

TABLE IV

GEOTHERMAL MANIFESTATION GROUP BASED ON THE GEOLOGICAL LINEAMENT PATTERN AND THE GEOMORPHIC INDICES CHARACTERISTIC OF THE STUDY AREA

Geothermal Manifestation Group	Geological Lineament Pattern	Geomorphic Indices Characteristic			
		Tectonic Deformation (R_b)	Landform Texture (D_d)	Tectonic Activity (S_{mf})	Lineament Density (L_d)
I	NNW-SSE NE-SW	Deformed (2.33)	Coarse (2.34)	Active (1.24)	High (1.68-2.52)
II	NNW-SSE NE-SW	Deformed (1.68-2.33)	Coarse (2.00-2.66)	Active (1.19-1.42)	Moderate (1.26-1.68)
III	NE-SW	Deformed (1.95-5.01)	Moderate (3.42-4.00)	Active (1.30-1.58)	High (1.68-2.52)
IV	NE-SW	Deformed (1.95)	Moderate (4.00)	Active (1.16-1.24)	Moderate (1.26-1.68)

1) Group I Geothermal Manifestation: The geothermal manifestations of group I are illustrated by yellow manifestation symbols in the overlay map. This group manifestations consist of the Songsang (SSG) and Garara (GRR) hot springs. The geothermal manifestations of this group appear in areas with the presence of: fault intersections with the north-northwest–south-southeast (NNW-SSE) and northeast-southwest (NE-SW) patterns, rock deformation with an R_b value of 2.33, coarse landform texture with a D_d value of 2.34 km/km², active tectonism with an S_{mf} value of 1.24, and high lineament density with the L_d values range from 1.68 to 2.52 km⁻¹. In brief, the group I geothermal manifestations appear on the Alluvial Fans (Qf) unit [6] at Sub-Watershed 9 (SW 9), which have undergone deformation due to active tectonism associated with relatively high rock permeability zone.

2) Group II Geothermal Manifestation: The geothermal manifestations of group II are illustrated by blue manifestation symbols in the overlay map. This group manifestations consist of the Padang Damar (PDM), Bukit Gadang (BGD), and Batu Bajanjang (BJJ) hot springs. The geothermal manifestations of this group appear in areas with the presence of: faults with the north-northwest–south-southeast (NNW-SSE) and northeast-southwest (NE-SW) patterns, rock deformations with the R_b values range from 1.68 to 2.33, coarse landform textures with the D_d values range from 2.00 to 2.66 km/km², active tectonisms with the S_{mf} values ranges from 1.19 to 1.42, and moderate lineament densities with the L_d values range from 1.26 to 1.68 km⁻¹. In brief, the group II geothermal manifestations appear on the Alluvial Fans (Qf) and Andesite of Gunung Talang (Qatg) unit [6] at Sub-Watershed 9 (SW 9), Sub-Watershed 10 (SW 10), and Sub-Watershed 14 (SW 14), which have undergone deformation due to active tectonism associated

with relatively moderate to high rock permeability zones.

3) Group III Geothermal Manifestation: The geothermal manifestations of group III are illustrated by purple manifestation symbols in the overlay map. This group manifestations consist of Bukit Kili (BKL) and Bawah Gunuang (BGN) hot springs. The geothermal manifestations of this group appear in areas with the presence of: faults with the northeast-southwest (NE-SW) pattern, rock deformations with the R_b values range from 1.95 to 5.01, moderate landform textures with the D_d values range from 3.42 to 4.00 km/km², active tectonisms with the S_{mf} values range from 1.30 to 1.58, and high lineament densities with the L_d values range from 1.68 to 2.52 km⁻¹. In brief, the group III geothermal manifestations appear on the Alluvial Fans (Qf) and Andesite of Gunung Talang (Qatg) unit [6] at Sub-Watershed 8 (SW 8) and Sub-Watershed 16 (SW 16), which have undergone deformation due to active tectonism associated with relatively moderate to high rock permeability zones.

4) Group IV Geothermal Manifestation: The geothermal manifestations of group IV are illustrated by black manifestation symbols in the overlay map. This group manifestations consist of Gabuo Atas (GBA) and Bawah Betung (BBT) hot springs. The geothermal manifestations of this group appear in areas with the presence of: faults with the northeast-southwest (NE-SW) pattern, rock deformation with an R_b value of 1.95, moderate landform texture with a D_d value of 4.00 km/km², active tectonism with the S_{mf} values range from 1.16 to 1.24, and moderate lineament density with the L_d values range from 1.26 to 1.68 km⁻¹. In brief, the group IV geothermal manifestations appear on Andesite of the Gunung Talang (Qatg) unit [6] at Sub-Watershed 16, which has undergone deformation due to active tectonism associated with relatively moderate rock permeability zones.

The distribution of the geothermal manifestation groups and their appearance characteristics are shown on the overlay map of geological lineament pattern and geomorphic indices characteristic of the study area (Figure 8).
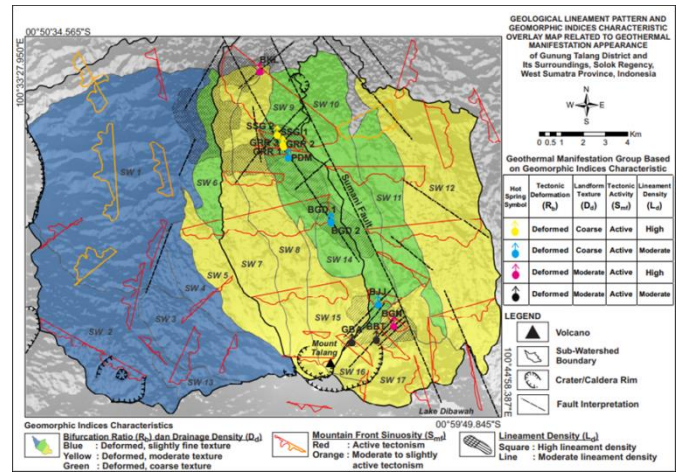

Figure 8: Geological lineament pattern and geomorphic indices characteristic overlay map shows the distribution of the geothermal manifestation groups and their appearance characteristics

IV. CONCLUSION

Gunung Talang District and its surroundings are generally covered with the Quaternary volcanic rocks which are deformed by the tectonic activity of the Sumatran Fault System. In this paper, we have presented a case study of the study area about the geological lineament pattern and geomorphic indices characteristics related to the appearance of geothermal manifestations. The results of remote sensing analysis suggest that the geological lineament patterns associated with the main geological structures in the study area are north-northwest–south-southeast (NNW-SSE) and northeast-southwest (NE-SW). These lineament patterns indicate synthetic and antithetic strike-slip faults around the Sumani Segment of Sumatran Fault System successively. In general, the results of quantitative analysis of geomorphic indices indicate deformed areas (R_b values: 1.14-5.45), coarse (D_d values: 2.00-2.66 km/km²),

moderate (D_d values: 3.14-4.00 km/km^2), and slightly fine landform textures (D_d values: 4.32-5.51 km/km^2), active (S_{mf} values: 1.05-1.64) and moderate to slightly active tectonisms (S_{mf} values: 1.74-2.52), and low (L_d values: 0.00-0.84 km^{-1}), moderate (L_d values: 0.84-1.68 km^{-1}), and high lineament densities (L_d values: 1.68-2.52 km^{-1}) over the study area. The evidence from the study integrated by the geospatial analysis implies that the geothermal manifestations in the study area are divided into four groups based on their appearance characteristics. These groups are group I (Songsang and Garara hot springs), group II (Padang Damar, Bukit Gadang, and Batu Bajanjang hot springs), group III (Bukit Kili and Bawah Gunuang hot springs), and group IV (Gabuo Atas and Bawah Betung hot springs). It is necessary to both confirm the results of this study and understand the subsurface condition of the study area through geological and geophysical field investigations in the future.

V. ACKNOWLEDGMENT

VI. REFERENCES

[1]. M. F. Umam, F. Muhammad, D. W. Adityatama, and D. P. Purba, "Tantangan pengembangan energi panas bumi dalam perannya terhadap ketahanan energi di Indonesia," Swara Patra, vol. 8, no. 3, September, 2018. [Online Serial]. Available: http://ejurnal.ppsdmmigas.esdm.go.id/sp/index.php/swarapatra/article/view/6. [Accessed: January 14, 2021].

[2]. D. Sukarna, "Development of geothermal policies, potential resources and implementation target," presented at Indo EBTKE Conference and Exhibition, Jakarta, Indonesia, 2012.

[3]. M. Boedihardi, A. Mulyono, A. Ginting, M. D. Mosby, and V. T. Radja, "Geology, energy potential and development of Indonesia's geothermal prospects," Bulletin of the Geological Sociecty of Malaysia, no. 33, p. 369, November 1993. [Abstract]. Available: AAPG Datapages, https://archives.datapages.com/data/geological-society-of-malaysia/bulletins/033/033001/pdfs/369.htm. [Accessed January 14, 2021].

[4]. A. F. Z and J. Hutahaean, "Penentuan struktur bawah permukaan tanah daerah potensi panas bumi dengan metode geomagnetik di Tinggi Raja Kabupaten Simalungun," Jurnal Einstein, vol. 3, no. 12, December, 2015. [Online Serial]. Available: https://jurnal.unimed.ac.id/2012/index.php/einsten/article/view/5444/8429. [Accessed: January 14, 2021].

[5]. L. Putriyana and H. Soekarno, "Numerical modelling of geothermal reservoir in Gunung Talang, West Sumatera, Indonesia," RISET Geologi dan Pertambangan, vol. 30, no. 1, June, 2020. [Online Serial]. Available: https://jrisetgeotam.lipi.go.id/index.php/jrisgeotam/article/view/1058. [Accessed: January 16, 2021].

[6]. P. H. Silitonga and Kastowo. Geological Map of the Solok Quadrangle, Sumatera, 2nd ed, scale 1:250.000. Bandung: Geological Research and Develompent Centre, 1995.

[7]. A. Munandar, E. Suhanto, D. Kusnadi, A. Idral, dan M. Solaviah, "Penyelidikan terpadu daerah panas bumi Gunung Talang Kabupaten Solok - Sumatera Barat," presented at Mineral Resources Inventory Activity Result Colloquium, Bandung, Indonesia, 2003.

[8]. K. Sieh and D. Natawidjaja, "Neotectonics of Sumatran Fault, Indonesia," Journal of Geophysical Research, vol. 105, no. B12, December, 2000. [Online Serial]. Available: https://agupubs.onlinelibrary.wiley.com/doi/abs/10.1029/2000JB900120. [Accessed: January 19, 2021].

[9]. D. Santoso, M. E. Suparka, S. Sudarman, and S. Suari, "The geothermal fields in central part of the Sumatra Fault Zone as derived from geophysical data," presented at World Geothermal Congress, Florence, Italy, 1995.

[10]. N. M. Saptadji, Teknik Panas Bumi. Bandung: ITB Press, 2001.

[11]. D. Burhan, "Pemetaan tipe mata air panas di Sumatera Barat (Studi kasus: 46 mata air panas di Kabupaten Pasaman, Pasaman Barat, Lima Puluh Kota, Agam, Tanah Datar, Solok, Sijunjung, dan Kabupaten Solok Selatan)," B.S. thesis, Dept. Phys., Univ. Andalas, Padang, Indonesia, 2017.

[12]. F. A. Rachmawati, A. D. Haryanto, J. Hutabarat, and M. Sumaryadi, "Penentuan sumber panas sistem panas bumi Gunung Api Talang, Sumatera Barat berdasarkan sejarah panas dan geokimia air," Padjadjaran Geoscience Journal, vol. 3, no. 1, February, 2019. [Online Serial]. Available: http://jurnal.unpad.ac.id/geoscience/article/view/20841. [Accessed: January 12, 2021].

[13]. S. Soengkono, "Te Kopia geothermal system (New Zealand)—the relationship between its structure and extent," Geothermics, vol. 28, no. 6, pp. 780-782, 1999.

[14]. S. Soengkono, "Analysis of digital topographic data for exploration and assessment of geothermal system," In Proc. 21st New Zealand Geothermal Workshop, 1999, pp. 163-166.

[15]. Suryantini and H. H. Wibowo, "Application of fault and fracture density (FFD) method for geothermal exploration in non-volcanic geothermal system: a case study in Sulawesi-Indonesia," In Proc. World Geothermal Congress, 2010, p. 1.

[16]. N. Sulaksana and A. H. Hamdani, "The analysis of remote sensing imagery for predicting structural geology in Berau Basin East Kalimantan," International Journal of Science and Research, vol. 3, no. 4, April, 2014. [Online Serial]. Available: https://www.ijsr.net/get_count.php?paper_id=20131349. [Accessed: January 21, 2021].

[17]. D. Hermawan dan Y. Rezky, "Delineasi daerah prospek panas bumi berdasarkan analisis kelurusan citra landsat di Candi Umbul-Telomoyo, Provinsi Jawa Tengah," Buletin Sumber Daya Geologi, vol. 6, no. 1, May, 2011. [Online Serial]. Available: http://buletinsdg.geologi.esdm.go.id/index.php/bsdg/article/view/92. [Accessed: January 21, 2021].

[18]. E. Sukiyah, Eds., Sistem Informasi Geografis: Konsep dan Aplikasinya dalam Analisis Geomorfologi Kuantitatif, 1st ed. Bandung: Unpad Press, 2017.

[19]. Peta Rupa Bumi Digital Indonesia, Badan Informasi Geospasial Republik Indonesia, 2015-2019. [Online]. Available: http://tanahair.indonesia.go.id/portal-web/. [Accessed: January 25, 2021].

[20]. ASTER Global Digital Elevation Model V003, NASA/METI/AIST/Japan Spacesystems and U.S./Japan ASTER Science Team, distributed by NASA EOSDIS Land Processes DAAC, 2019, [Online]. Available: https://doi.org/10.5067/ASTER/ASTGTM.003. [Accessed: January 25, 2021].

[21]. J. P. Richards, "Lineaments revisited," Society of Economic Geologists Newsletter, vol. 42, no. 1, pp. 14-20, 2000.

[22]. L. Q. Hung, O. Batelaan, and F. D. Smedt, "Lineament extraction and analysis, comparison of LANDSAT ETM and ASTER imagery. Case study: Suoimuoi tropical karst catchment, Vietnam," In Proc. SPIE, presented at the Remote Sensing for Environmental Monitoring, GIS Applications, and Geology, SPIE, 2005, p. 59830T-1.

[23]. Jamal, N. Sulaksana, E. Sukiyah, and Y. A. Sendjaja, "Analisis multi raster SRTM, radarsat dan landsat untuk karakterisisasi morfo-struktur dari geometri sesar di Daerah Binuang, Kalimantan Selatan, Jurnal Geologi dan Sumberdaya Mineral, vol. 20, no. 1, February, 2019. [Online Serial]. Available: https://jgsm.geologi.esdm.go.id/index.php/JGSM/article/view/405. [Accessed: January 27, 2021].

[24]. P. A. Allen and J. R. Allen, Basin Analysis: Principles and Applications, 2nd ed. Malden, MA: Blackwell Publishing, 2005.

[25]. H. T. Verstappen, Applied Geomorphology: Geomorphological Surveys for Environmental Development. New York: Elsevier Science Publishing Company Inc, 1983.

[26]. R. E. Horton, "Erosional development of stream and their drainage basins: a hydrophysical approach to quantitative morphology," Geological Society of America Bulletin, vol. 56, no. 3, p. 283, 1945.

[27]. E. Sukiyah, "The erosion model of the Quarternary volcanic terrain in southern part of Bandung Basin," Ph.D. dissertation, Dept. Geol. Eng., Univ. Padjadjaran, Sumedang, Indonesia, 2009.

[28]. D. Gentana, N. Sulaksana, E. Sukiyah, and E. T. Yuningsih, "Index of active tectonic assessment: quantitative-based geomorphometric and morphotectonic analysis at Way Belu Drainage Basin, Lampung Province, Indonesia,"

International Journal of Advanced Science Engineering Information Technology, vol. 8, no. 6, December, 2018. [Online Serial]. Available: http://www.insightsociety.org/ojaseit/index.php/ijaseit/article/view/6089. [Accessed: February 2, 2021].

[29]. W. B. Bull and L. D. McFadden, "Tectonic geomorphology north and south of the Garlock fault, California," in Geomorphology in Arid Regions. Proceedings of the Eighth Annual Geomorphology Symposium, 1st ed., D. O. Doehring, Eds. New York: Routledge, 1997, pp. 115-137.

[30]. N. Sulaksana, Supriyadi, Ismawan, P. P. R. Rendra, and M. Sulastri, "Active fault analysis through quantitative assesment method in Cikapundung Sub Watershed," International Journal of Scientific Research in Science and Technology, vol. 3, no. 6, July, 2017. [Online Serial]. Available: https://ijsrst.com/IJSRST173634. [Accessed: February 5, 2021].

[31]. J. C. Doornkamp, "Geomorphological approaches to the study of neotectonics," Journal of the Geological Society, 143, pp. 335-336, 1986.

[32]. D. Gentana, N. Sulaksana, E. Sukiyah, and E. T. Yuningsih, "Morphotectonics of Mount Rendingan Area related to the appearances of geothermal surface manifestations," Indonesian Journal on Geoscience, vol. 6, no. 3, December, 2019. [Online Serial]. Available: http://ijog.bgl.esdm.go.id/index.php/IJOG/article/view/509. [Accessed: February 8, 2021].